COBEM 2023 27TH INTERNATIONAL CONGRESS OF MECHANICAL ENGENEERING

ABCM Brazilian Society of Mechanical Sciences and Engineering
27th ABCM International Congress of Mechanical Engineering
December 04-08, 2023, Florianópolis-SC, Brazil

COB-2023-0667
COMPARATIVE ANALYSIS OF THE BIOMECHANICAL BEHAVIOR OF TWO TYPES OF SOLUTIONS USED FOR THE TREATMENT OF BUSH-HOFFA FRACTURES

João Marcos Guimarães Rabelo
Post-Graduation Program in Structural Engineering, Federal University of Minas Gerais, Brazil,
Department of Computing and Civil Engineering, Federal Center for Technological Education of Minas Gerais (CEFET-MG), Brazil, Address: Av. dos Imigrantes, 1000 - Jardim Panorama, Varginha - MG. Zip Code: 37022-560.
e-mail:joao.rabelo@engenharia.ufjf.br

Robinson Esteves Pires
Department of Locomotor System, Federal University of Minas Gerais, Brazil, Address: Av. Antonio Carlos, 6627, Campus Pampulha, Belo Horizonte – MG. Zip Code: 31270-901.
e-mail: robinsonestevespires@gmail.com

Armando Belato Pereira
Department of Computing and Civil Engineering, Federal Center for Technological Education of Minas Gerais (CEFET-MG), Brazil, Address: Av. dos Imigrantes, 1000 - Jardim Panorama, Varginha - MG. Zip Code: 37022-560.
e-mail: armandobelato@cefetmg.br

Raphael Lúcio Reis dos Santos
Department of transport and geotechnics, Federal Center for Technological Education of Minas Gerais (CEFET-MG), Brazil,
e-mail:, raphael.santos@cefetmg.br.

Estevam Barbosa de Las Casas
Carlos Alberto Cimini Junior
Department of Structural Engineering, Federal University of Minas Gerais, Brazil, Address: Av. Antonio Carlos, 6627, Campus Pampulha, Belo Horizonte – MG. Zip Code: 31270-901.
e-mail: estevam@dees.ufmg.br, carloscimini@gmail.com

Abstract. *Surgical treatment of Bush-Hoffa fractures is still controversial, since a treatment protocol has not been defined. The objective of this study is to evaluate, through finite element analysis, the biomechanical behavior of two surgical solutions that use screws with a posterior-to-anterior and anterior-to-posterior approach, commonly used in the literature for the treatment of Bush-Hoffa type I fractures. Under the conditions of vertical shear loading, the displacements along the femur axis, the von Mises stresses and the absolute maximum and minimum stresses in the bone were evaluated. The values found for the displacements were 1.536 mm and 1.225 mm and the von Mises stresses of 555.537 MPa and 700.357 MPa for the posterior-to-anterior and anterior-to-posterior approaches, respectively. The solution with the use of two 4.5 mm cannulated screws from anterior to posterior presented the satisfactory results evaluated for mechanical behavior.*

Keywords: *coronal fractures, femur fractures, finite elements, biomechanical behavior, Bush-Hoffa Fractures*

1. INTRODUCTION

Fractures of the femoral condyles are extremely rare and occur due to high-energy trauma (Freitas et al., 2021; Onay et al., 2018; Pires et al., 2018). The first description of femoral condyle fracture in the coronal plane was credited to Friedrich Busch in 1869 (Bartoníček & Rammelt, 2015; Busch & Fall, 1869). Later, Albert Hoffa (Hoffa, 1904), in 1888, defined this type of fracture as an intra-articular unicondylar type in the coronal plane of the distal end of the femur. These fractures occur more commonly on the lateral condyle than on the medial condyle (Arastu et al., 2013; Orapiriyakul et al., 2018). Fracture patterns were subsequently classified by Letenneur into Type I, II and III according to the configuration of the fragment (Letenneur et al., 1978; Pires et al., 2018). Among the three reported types, type I is the most frequent occurrence (Xie et al., 2017).

The treatment of Busch-Hoffa fractures basically consists of anatomical reduction of the fracture, with restoration of the joint surface and fixation with the principle of absolute stability to allow early joint mobilization. The usual treatment techniques reported in the literature employ screws perpendicular to the fracture line in the coronal plane. The screws used to fix Busch-Hoffa fractures vary from mini-fragment implants, cortical screws or cannulated screws, depending on

the size of the fractured fragment, the location and the preference of the surgeon. Despite reports of this studies of fixation techniques in the literature, there is still no consensus on the best method, or even on the configuration of the intervention (Jarit et al., 2006; Patel & Tejwani, 2018; Zhou et al., 2019). The characteristic of the fracture design and the associated injuries are crucial aspects to delineate the surgical treatment plan.

The treatment of this type of fracture must, therefore, consider a structural rigidity capable of fixing the fragment with absolute stability. Still, the academic literature leaves inconclusive the question about the best surgical approach, whether it should attend to an anterior or posterior access route, this definition of treatment is extremely important from the point of view of the possibility of causing neurovascular injuries (Jarit et al., 2006; Yao et al., 2020).

One of the classic and common stabilization methods consists of using cannulated screws in the anterior to posterior direction and in the posterior to anterior direction (Orapiriyakul et al., 2018). Therefore, the main objective of this study is to evaluate and compare the biomechanical performance related to displacements of the fragment originating from a Hoffa Type I fracture treated with an anterior approach versus a posterior approach, using 4.5x65 mm cannulated screws in the anterior-posterior and posterior-anterior direction as an example of intervention. It is noteworthy that biomechanical studies via Finite Elements are rare in the literature for this type of fracture (Freitas et al., 2021) where this work seeks to contribute by evaluating the mechanical performance regarding anterior and posterior approaches.

It is reported in the scientific literature that the anterior-to-posterior approach technique, from a surgical point of view, is easy to access and perform (Arastu et al., 2013), whereas the posterior approach is more difficult, which may endanger neurovascular structures and increase chances of damaging the articular cartilage (Jarit et al., 2006), and this point of view is very important to be considered when choosing the approach.

2. METHODOLOGY

2.1 Dimensional characteristics

The finite element model for the synthetic bone was created from digital images (DICOM) file obtained from a computed tomography scan of a synthetic bone sample (Sawbone Model 3403-102, 20 PCF, Pacific Research Laboratories, Inc., Vashon, WA, USA). The fracture was reproduced as a 1 mm thick cut without creating space between the fracture and the bone, extending towards the posterior cortex of the distal femoral metaphysis, thus representing a type I Hoffa Fracture, classification 33-B3.2 according to AO/OTA (Marsh et al., 2007; Martinet et al., 2000; Onay et al., 2018). The cannulated screws applied for the surgical treatment were modeled according to the dimensional characteristics of the manufacturer, having the dimensions of 4.5x65 mm. Their mechanical properties correspond to the alloy Ti-6Al-4V, observing the NBR ISO 5832-3 (NBRISO5832-3, 2022) standard and the values provided by the manufacturer (OCX®, São Paulo – SP, Brazil).

The insertion observed the tracing obtained in a radiographic image of an experimentally studied sample for the anterior-posterior direction. For the creation of the posterior-anterior model, the same line of tracing of the screws was observed for their positioning. Also, only the distal region of the femur was considered, in order to simplify the analysis, evaluating the first 120 mm from the distal condylar end.

Figure 1 illustrates the positioning of the implants and the section of the fracture studied.

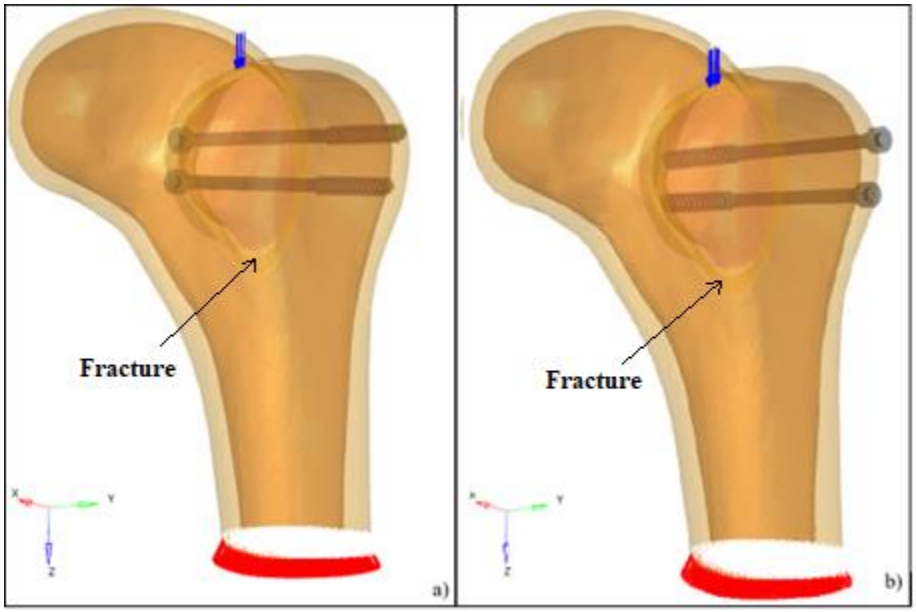

Figure 1. Geometric characteristic of the studied model; a) Postero-anterior, b) Antero-posterior.

2.2 Characteristics of the Finite Element models

All materials were assumed to be homogeneous, isotropic and linear elastic, as long as its geometric limits are respected. The mechanical properties inserted in the numerical model were the Young's modulus (Luo et al., 2022; NBRISO5832-3, 2022) and Poisson ratio, presented in Table 1. The values considered were those informed by the manufacturer's catalog for the synthetic bone and researched in the literature for the screws that are manufactured in Ti-6Al-4V.

Table 1 - Mechanical properties considered in the model (t = tension, c = compression).

Material	Young`s modulus (N/mm²)	Poisson ratio	Ultimate strength (MPa)
Cortical bone	16.000	0,30	157 (t) /106 (c)
Trabecular bone	210	0,30	210 (t) / 284 (c)
Screw Ti-Al-4V	115.000	0,34	860 (t)

For the delimitation of the loading conditions, a static incremental load (ten increments) represented by a pressure force of magnitude resultant equal to 1000 N was applied in the direction of the cartesian Z axis (blue arrows, Figure 1), at the upper face of the fractured segment near the fracture line. The magnitude of 1000 N was chosen to compare with the results obtained with those performed by experiments carried out by (Sun et al., 2017). The model was considered fixed in the base, with restricted translation in the three cartesian axises (red triangles, Figure 1).

A very important stage of the analysis was to evaluate and consider the contact between the geometric parts of the model. The contact interaction between the fracture and the bone was evaluated as slippery, without penetration and without friction. This consideration is valid, since the mobility situation just after surgery has not yet allowed for bone consolidation. The interaction between the screw and the bone was evaluated as a contact with friction, however, without penetration. The unfasten of the screw with the bone is also considered. The coefficient of friction between the screw and the bone was considered equal to 0.30 (Zeng et al., 2020).

Mesh generation was performed using the Hypermesh™ program to construct the finite element mesh, assign the material properties (as shown in Fig. 1 and Table 1) and define the boundary conditions. The element used was the 4-node linear tetrahedron, the choice of the linear tetrahedron is due to the fact of the complex geometry that is the condylar region of the femur, where the format of this finite element manages to better discretize the geometry variation. The mesh was created with edge elements of approximately 2 mm receiving refinement around the screws, where the elements had edges of around 0.5 mm, the screws were also generated with edge elements of approximately 0.5 mm. With the model definitions, it was exported for resolution in the Optistruct™ solver.

This analysis, therefore, was geometric non-linear, where the desired values to be obtained were the relative vertical displacement between the movement of the fracture and the rest of the femur bone, the maximum Von Mises stress on the screw and the maximum (traction) and minimum (compression) principal stresses absolute in bone and fracture.

3. RESULTS

3.1 Description of vertical displacements

The stiffness of the fracture stabilizing solution was evaluated through the distribution of vertical displacements (Z axis) along the finite elements of the fracture and bone, being found a maximum displacement value of 1.536 mm for an approach with screws from posterior to anterior (Figure 2a) and 1.225 mm for an anterior-to-posterior screw approach (Figure 2b). The comparison between the two approaches shows a 25.39% smaller displacement in the approach with the screws applied from anterior to posterior. The displacements found were more significant along the fracture than in the body of the bone in both of cases, due to the sliding of the fracture at the interface with the bone. This displacement is counteracted by the rigidity caused by the use of screws.

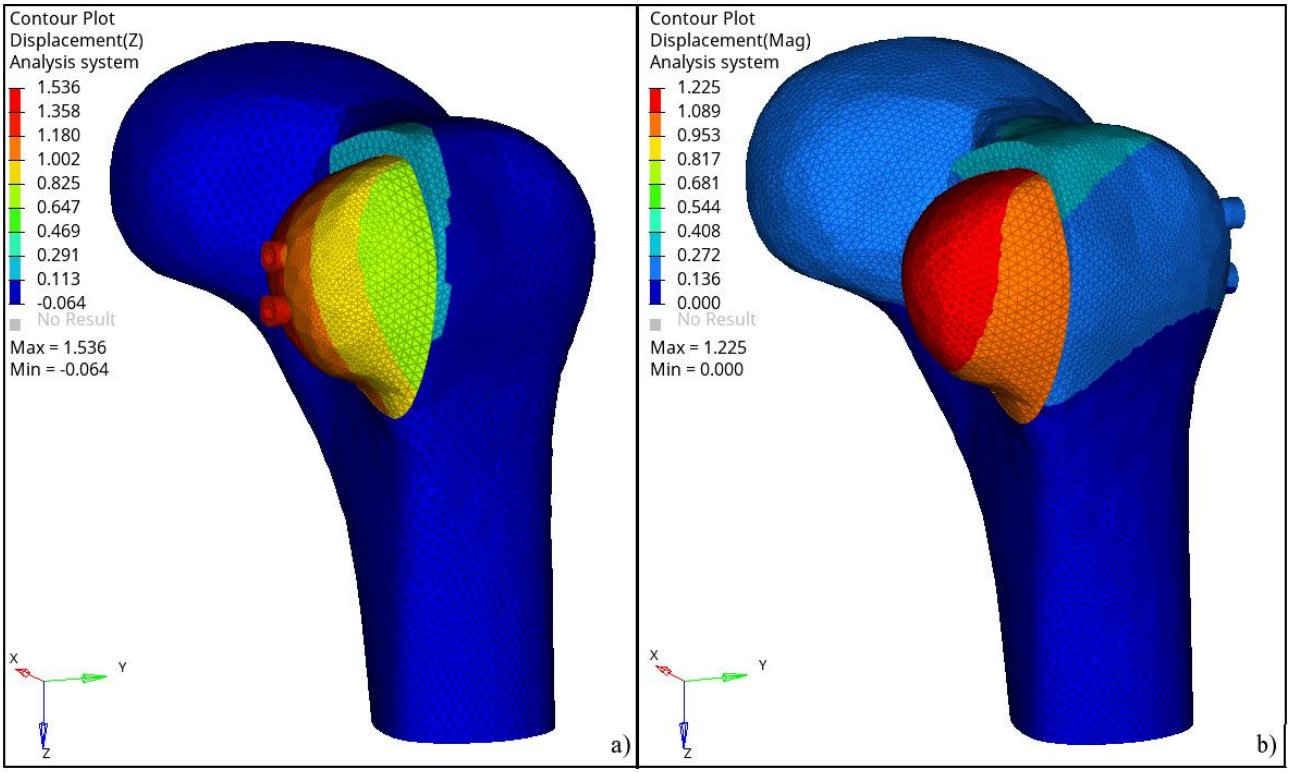

Figure 2. Distribution of vertical displacements along the model with scale factor of five for better visualization; a) Postero-anterior, b) Antero-posterior.

3.2 Distribution of absolute principal stresses

The absolute maximum principal stresses found in the bone in the region of the orifice were within a range between 50 MPa and -50 MPa for the posteroanterior approach and anteroposterior approach. Figure 3 illustrates the stress distribution along the hole on the bone face, in contact with the fracture. It can be seen that there was a predominance of compressive stresses in the lower part of the hole and no significant stresses in the upper part, this is due to the displacement of the screw in relation to the bone in the contact modeling, which faithfully represents reality.

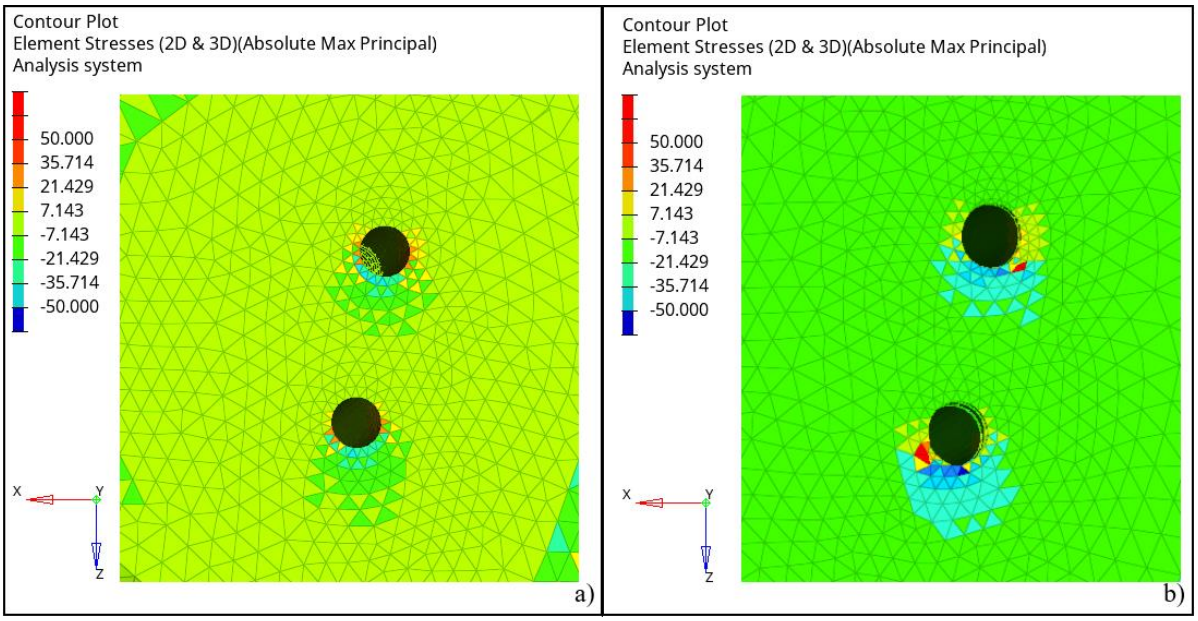

Figure 3. Distribution of principal stresses on the face of the bone in contact with the fracture; a) Postero-anterior, b) Antero-posterior.

The distribution of maximum principal stresses found in bone fracture in the hole region is represented by Figure 4 along the hole on the face of the bone, in contact with the fracture. It can be seen that there was a predominance of compressive stresses in the lower part of the hole and there were no significant stresses in the upper region of the hole, the upper part being the most distal location. Stresses with absolute values greater than 75 MPa were not found on the contact face. This distribution is inverse to the distribution observed on the face of the bone, since it is a shear movement between the fracture and the bone.

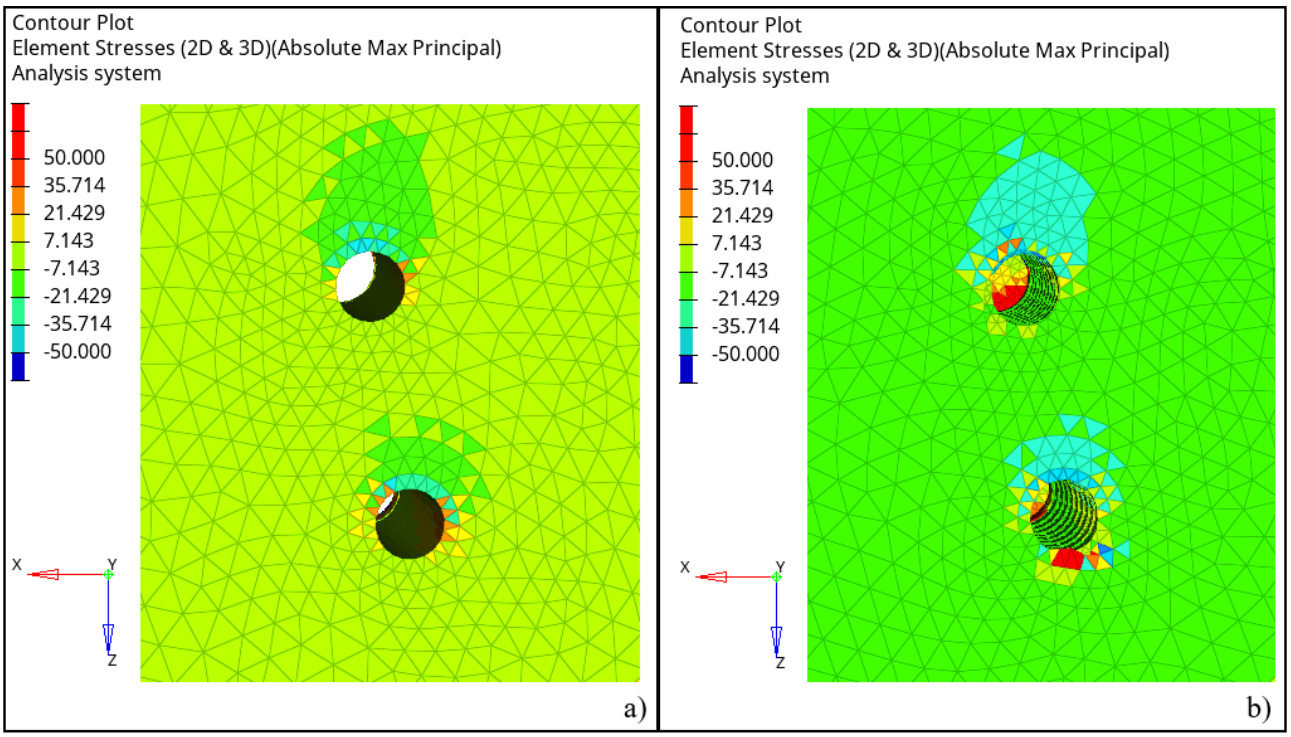

Figure 4. Distribution of principal stresses on the fracture face in contact with the bone; a) Postero-anterior, b) Antero-posterior.

Stress peaks above 50 MPa are observed in the bone and in the fracture in the region of the screw thread and web. The maximum values resisted by the synthetic bone for traction and compression efforts are, respectively: 157 MPa and 106 MPa for the cortical part and 210 MPa and 284 MPa for the trabecular part (Sawbone Model 3403-102, 20 PCF, Pacific Research Laboratories, Inc., Vashon, WA, USA).

3.3 Von Mises stress distribution in screws

The von Mises stress distribution was evaluated to verify whether the stresses acting along the screw are within the acceptable limits of resistance, which according to the manufacturer's data, the limit of resistance to flow is 888 MPa (OCX®, São Paulo – SP, Brazil). Figure 5 illustrates the stress distribution for the screws, with a maximum value of 555.537 MPa for posterior to anterior use and 700.357 MPa for anterior to posterior use. The von Mises stress values found in the screws for the anterior posterior approximation were 26.07% greater than the values found for the posterior anterior approximation.

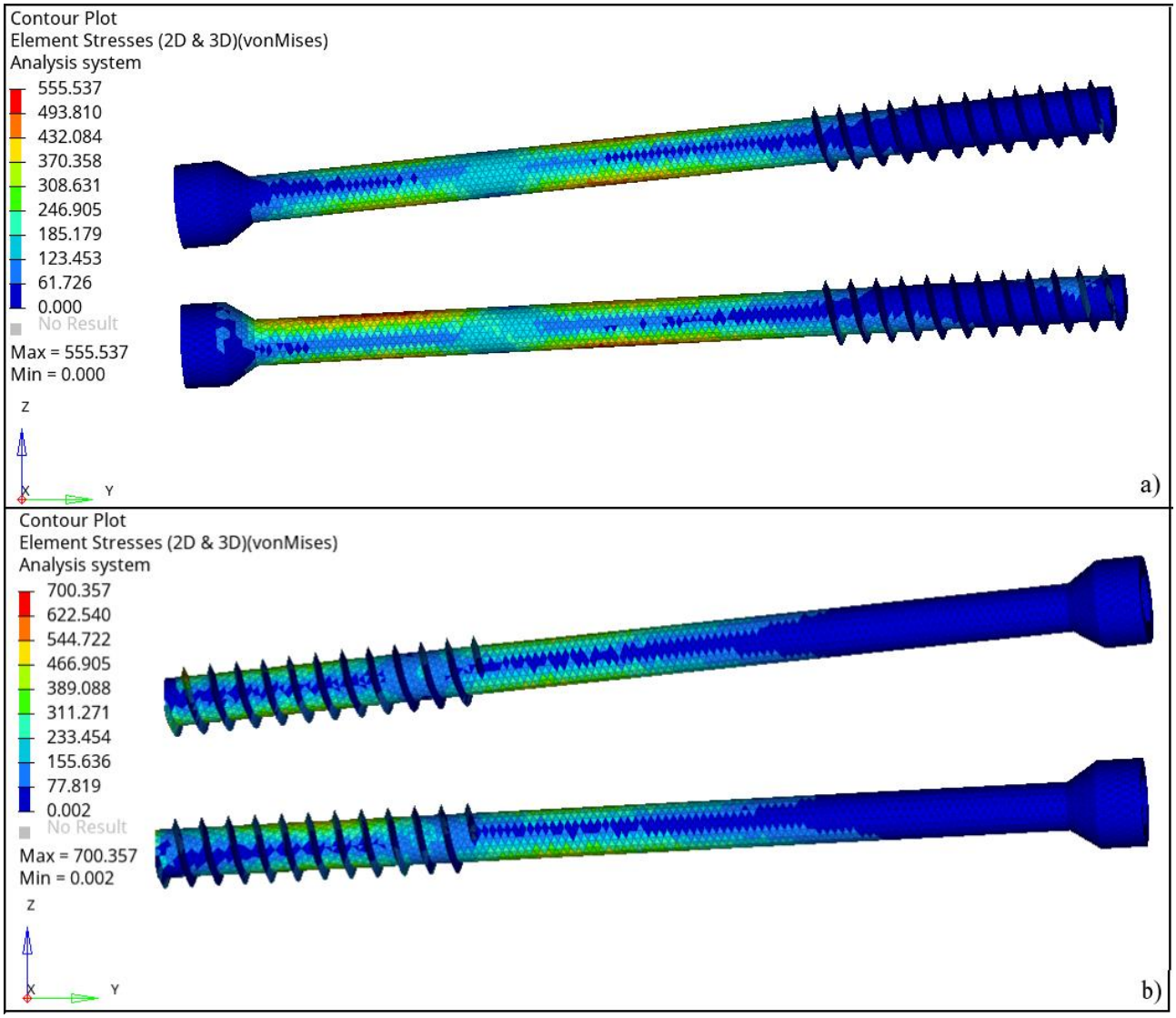

Figure 5. Distribution of von Mises stresses on implanted screws; a) Postero-anterior, b) Antero-posterior.

4. DISCUSSION

The correct treatment and diagnosis for Bush-Hoffa fractures are still a challenge in the clinical context (Xu et al., 2016; Zhou et al., 2019). The most common and simplistic solutions used in the literature are the use of cannulated screws in different directions and different approaches. The main contribution of this study was to evaluate the stabilization conditions of the proposed solutions, highlighting important aspects such as fracture displacement, screw resistance and the stresses involved in the bone in the region of contact with the screw. Clinical considerations are also relevant for the choice of the best treatment.

The present biomechanical study analyzed the use of two 4,5x65 mm cannulated screws in the posterior to anterior (PA) and anterior to posterior (AP) directions for the treatment of type I Hoffa fractures. The PA solution showed a greater displacement than the AP solution, when compared to the experimental study carried out by (Sun et al., 2017), this information was reaffirmed, where the author found 2,835 mm for the PA approach and 2,292 mm for the AP approach for a load of 1000 N.

A direct comparison between the numerical model and the experimental values found is not possible, because the test conditions involve accommodation of the specimen (this fact justifies smaller displacements found), in addition to the experimental displacement being measured between two horizontal points on the lateral face of the sample, while our numerical analysis demonstrates the displacement variation along the fracture, the maximum displacement being presented only for purposes of comparison between the models.

Still, with regard to the displacement in question, as observed by (Egol et al., 2004), stability determines the deformation at the fracture site, and the deformation determines the type of healing that can occur at the fracture site, the

ideal for bone consolidation being a deformation not exceeding 10%. Our values found 1.536 mm and 1.225 mm representing 3.15% and 2.52% of deformation, since the fracture has an average length of 48.7 mm.

In this analysis, the behavior of the displacements along the screws was also observed to evaluate the influence of considering the contact at the interface of the different materials. The detachment of the screw from the bone was observed as the displacements progressed, being clearer in the region without the screw thread. Through this behavior, we can infer that the thread contributes more significantly to reducing the displacement of the screw along the bone, which probably contributed to reducing the displacements found in the anterior to posterior approximation, since the region of the thread is in the fracture and this helps causing the fracture to "slip less" along the screw.

Regarding the absolute principal stresses found in the thread region on the fracture and bone face, these did not exceed the material's rupture stresses. Knowledge of stresses in this region is important, as (Egol et al., 2004) observed that high stresses that exceed bone strength led to bone failure or bone absorption and subsequent loosening of the screw. Therefore, the solutions studied do not present a risk of failure due to the adhesion of the screw to the bone at first for a load of 1000 N.

The third analysis observed the von Mises tensions acting on the screw to evaluate the safety of the implants in relation to their resistance against the requests, observing the results found, it can be stated that the AP direction presents greater stress on the implants, however, the stress found corresponds to 78.87% of the maximum resisted by the material informed by the manufacturer, which does not present a risk of failure for a load of 1000 N.

In this scenario, our results showed that an anterior approach using a lateral route, using screws from anterior to posterior, presented better results in the evaluated aspects, which was also observed in the experimental study by (Sun et al., 2017). This solution has also clinical preference due to the fact that it is easier to perform, reducing the possibility of damage to the articular cartilage and neurovascular. This evaluation requires clinical and experimental tests to provide higher levels of evidence, producing an interface between medicine and engineering through the comparison between biomechanical behavioral studies techniques and techniques of clinical surgical approaches.

It is observed that in terms of biomechanical studies, the methodology using finite elements allowed an evaluation of important aspects of the behavior of this stabilized fracture with a different surgical approach, such as the evaluation of the resistance capacity of the bone at the bone-screw interface and the tensions acting along of the implant, which allows a greater understanding of the problem from a microstructural aspect, where experimental tests would have difficulty representing with greater scope and precision, being limited, in most cases, to obtaining the vertical displacement, which was also evaluated.

It should also be remembered that the analyzed model was simplified because it did not consider the contribution of soft parts (ligaments, muscles), given the difficulty of predicting the behavior of these structures, although they contribute to stability (Mäkinen et al., 2015). We also emphasize that the properties taken from the literature, such as coefficient of friction and Young's modulus of the implants used, may not exactly correspond to the properties of the materials used in the experiments carried out by (Sun et al., 2017).

Finally, the development of the methodology of the present study for this type of fracture is rare in the literature and serves as a basis for the creation of new analyzes capable of evaluating the influence of the position and diameter of the screws, as well as the use of screws with full thread. In addition, these numerical studies must be aligned with medical knowledge to decide on the choice of techniques that optimize surgical time, reduce surgical risks and lead to better postoperative recovery.

5. FINAL CONSIDERATION

The solution of applying 4.5x65 mm cannulated screws from anterior to posterior showed the best mechanical results via Finite Elements with the smallest vertical displacement and has a von Mises stress acting on the implants lower than the yield stress for the material, to the models considered in the treatment of Type I Hoffa fractures. The maximum tensile and minimum compressive stresses acting on the bone did not exceed the limit resisted by the material, not presenting a risk of screw loosening.

This study aims to contribute to the interface between engineering and medicine in the academic community and provide support for further studies on Hoffa fractures, making it possible to consider and evaluate in the model the different mechanical properties for an individual model, dependent of the variation in bone densitometry (that can be obtained in CT scans), and also to evaluate the behavior of the fixation when submitted to different loads of the gait cycle during the patient's recovery.

6. ACKNOWLEDGEMENTS

Authors would like to acknowledge the support of CAPES, UFMG, CNPq, FAPEMIG and CEFET-MG.

7. REFERENCES

Arastu, M. H., Kokke, M. C., Duffy, P. J., Korley, R. E. C., & Buckley, R. E. (2013). Coronal plane partial articular fractures of the distal femoral condyle. *The Bone & Joint Journal*, *95-B*(9), 1165–1171. https://doi.org/10.1302/0301-620X.95B9.30656

Bartoníček, J., & Rammelt, S. (2015). History of femoral head fracture and coronal fracture of the femoral condyles. *International Orthopaedics*, *39*(6), 1245–1250. https://doi.org/10.1007/s00264-015-2730-x

Busch, F., & Fall, V. (1869). Mehrere Fälle seltener Knochenverletzungen. *Arch Klin Chir*, *10*, 703–719.

Egol, K. A., Kubiak, E. N., Fulkerson, E., Kummer, F. J., & Koval, K. J. (2004). Biomechanics of Locked Plates and Screws. *Journal of Orthopaedic Trauma*, *18*(8), 488–493. https://doi.org/10.1097/00005131-200409000-00003

Freitas, A., Aquino, R. J., de Brito, F. F., Bonfim, V. M., Júnior, J. V. T., & Daher, W. R. (2021). Analysis of mechanical variables in Hoffa fracture – A comparison of four methods by finite elements. *Journal of Clinical Orthopaedics and Trauma*, *14*, 101–105. https://doi.org/10.1016/j.jcot.2020.07.032

Hoffa, A. (1904). Lehrbuch der Frakturen und Luxationen, IV. *Aufl. Stuttgart: Ferdinand Enke.*

Jarit, G. J., Kummer, F. J., Gibber, M. J., & Egol, K. A. (2006). A Mechanical Evaluation of Two Fixation Methods Using Cancellous Screws for Coronal Fractures of the Lateral Condyle of the Distal Femur (OTA type 33B). *Journal of Orthopaedic Trauma*, *20*(4), 273–276. https://doi.org/10.1097/00005131-200604000-00007

Letenneur, J., Labour, P. E., Rogez, J. M., Lignon, J., & Bainvel, J. V. (1978). [Hoffa's fractures. Report of 20 cases (author's transl)]. *Annales de Chirurgie*, *32*(3–4), 213–219.

Luo, X., Wang, Y., Dang, N., Tian, K., Wang, K., Zhao, C., Zha, X., Wang, X., & Yu, Y. (2022). Gradient microstructure and foreign-object-damaged fatigue properties of Ti6Al4V titanium alloy processed by the laser shock peening and subsequent shot peening. *Materials Science and Engineering: A*, *849*, 143398. https://doi.org/10.1016/j.msea.2022.143398

Mäkinen, T. J., Dhotar, H. S., Fichman, S. G., Gunton, M. J., Woodside, M., Safir, O., Backstein, D., Willett, T. L., & Kuzyk, P. R. T. (2015). Periprosthetic supracondylar femoral fractures following knee arthroplasty: a biomechanical comparison of four methods of fixation. *International Orthopaedics*, *39*(9), 1737–1742. https://doi.org/10.1007/s00264-015-2764-0

Marsh, J. L., Slongo, T. F., Agel, J., Broderick, J. S., Creevey, W., DeCoster, T. A., Prokuski, L., Sirkin, M. S., Ziran, B., Henley, B., & Audigé, L. (2007). Fracture and Dislocation Classification Compendium - 2007. *Journal of Orthopaedic Trauma*, *21*(Supplement), S1–S6. https://doi.org/10.1097/00005131-200711101-00001

Martinet, O., Cordey, J., Harder, Y., Maier, A., Bühler, M., & Barraud, G. E. (2000). The epidemiology of fractures of the distal femur. *Injury*, *31*, 62–94. https://doi.org/10.1016/S0020-1383(00)80034-0

NBRISO5832-3. (2022). *Implantes para cirurgia - Materiais metálicos - Parte 3: Liga conformada de titânio 6-alumínio 4-vanádio*.

Onay, T., Gülabi, D., Çolak, İ., Bulut, G., Gümüştaş, S. A., & Çeçen, G. S. (2018). Surgically treated Hoffa Fractures with poor long-term functional results. *Injury*, *49*(2), 398–403. https://doi.org/10.1016/j.injury.2017.11.026

Orapiriyakul, W., Apivatthakakul, T., & Buranaphatthana, T. (2018). How to determine the surgical approach in Hoffa fractures? *Injury*, *49*(12), 2302–2311. https://doi.org/10.1016/j.injury.2018.11.034

Patel, P. B., & Tejwani, N. C. (2018). The Hoffa fracture: Coronal fracture of the femoral condyle a review of literature. *Journal of Orthopaedics*, *15*(2), 726–731. https://doi.org/10.1016/j.jor.2018.05.027

Pires, R. E., Giordano, V., Fogagnolo, F., Yoon, R. S., Liporace, F. A., & Kfuri, M. (2018). Algorithmic treatment of Busch-Hoffa distal femur fractures: A technical note based on a modified Letenneur classification. *Injury*, *49*(8), 1623–1629. https://doi.org/10.1016/j.injury.2018.06.008

Sun, H., He, Q.-F., Huang, Y.-G., Pan, J.-F., Luo, C.-F., & Chai, Y.-M. (2017). Plate fixation for Letenneur type I Hoffa fracture: a biomechanical study. *Injury*, *48*(7), 1492–1498. https://doi.org/10.1016/j.injury.2017.03.044

Xie, X., Zhan, Y., Dong, M., He, Q., Lucas, J. F., Zhang, Y., Wang, Y., & Luo, C. (2017). Two and Three-Dimensional CT Mapping of Hoffa Fractures. *Journal of Bone and Joint Surgery*, *99*(21), 1866–1874. https://doi.org/10.2106/JBJS.17.00473

Xu, Y., Li, H., Yang, H., & Pan, Z. (2016). A comparison of the clinical effect of two fixation methods on Hoffa fractures. *SpringerPlus*, *5*(1), 1164. https://doi.org/10.1186/s40064-016-2861-6

Yao, S.-H., Su, W.-R., Hsu, K.-L., Chen, Y., Hong, C.-K., & Kuan, F.-C. (2020). A biomechanical comparison of two screw fixation methods in a Letenneur type I Hoffa fracture. *BMC Musculoskeletal Disorders*, *21*(1), 497. https://doi.org/10.1186/s12891-020-03527-4

Zeng, W., Liu, Y., & Hou, X. (2020). Biomechanical evaluation of internal fixation implants for femoral neck fractures: A comparative finite element analysis. *Computer Methods and Programs in Biomedicine*, *196*, 105714. https://doi.org/10.1016/j.cmpb.2020.105714

Zhou, Y., Pan, Y., Wang, Q., Hou, Z., & Chen, W. (2019). Hoffa fracture of the femoral condyle. *Medicine*, *98*(8), e14633. https://doi.org/10.1097/MD.0000000000014633

8. RESPONSIBILITY NOTICE

The authors are the only responsible for the printed material included in this paper.